Chapter 4

HAZ Phase Transformation and Thermal Damage for Laser Remanufacturing a High-Strength Stainless Steel

Shi-yun Dong, Xiang-yi Feng, Jin-xiang Fang and Shi-xing Yan

Additional information is available at the end of the chapter

http://dx.doi.org/10.5772/intechopen.79910

Abstract

It briefly introduced laser remanufacturing, which was an advanced repairing method to refabricate damaged components based on laser forming technologies. The possible factors in determining the performance of the laser remanufacturing FV520B were studied by numerical simulation and experimental methods. First, the results of free dilatometry test showed that the volume effect of phase transformations were corresponding to the transformation temperatures and heating rate of the laser process had remarkable effects on the kinetics of phase transformation. In addition, the evolution of temperature fields of the single-pass and multi-layer laser cladding processes were analyzed by numerical simulation method based on deactivate and reactivate element theory. A combined method of dilatometry and metallography was conducted to reveal the effect of cooling condition and phase transformation on the microstructure of HAZ. The maximum temperature of thermal cycle had a dominating effect on the microstructure, microhardness and phase transformation temperature rather than cooling rate. Thermal cycles had a significant effect on the metallographic transformation and consequently decided the mechanical performance. Microhardness and tensile tests were conducted and the results showed that strength and ductility of laser remanufacturing FV520B were equivalent to that of forgings.

Keywords: phase transformation, laser remanufacturing, heat-affected zone, martensite stainless steel

1. Introduction

Conventional high strength steel (CHSS) has been defined in advanced high-strength steels (AHSS) Application Guideline 3.0 by World Steel Association (IISI) as steel material with high

strength (yield strength ≥ 210 MPa and tensile strength ≥ 370 MPa). In recent years, light alloy like aluminum and magnesium alloys were widely used in automobile lightening and it also promotes the emergence and development of the AHSS. As a typical example of high strength steels, martensitic stainless steel with good comprehensive mechanical properties, casting performance and excellent corrosion resistance was used in various large-scale and complex operating conditions equipment, such as large-scale compressor rotors, air-compressor blade and structural components of the nuclear reactor. These high performance parts with complicated structure and high manufacturing cost had great potential to remanufacture. The suitable material testing technique and perfect remanufacturing process were desperately needed for the remanufacturing of damaged equipment and it is environmentally friendly, more economical and efficient.

The laser cladding processing is an advanced high-energy beam remanufacturing techniques. As the light source, laser beam had high energy-density, high-precision and high flexible processing to achieve net shaping forming for manufacturing those structural parts or components with complex inner structure [1]. Taking full advantages of laser beam and based on the laser cladding, laser remanufacturing technology was used for remanufacturing the disabled parts of the damaged equipment and the original shape or external dimensions recovered accurately after proper subsequent machining. Meanwhile, the alloy powder material and the matrix of the work-piece produce high quality metallurgically bonding under heating of powerful laser during the remanufacturing processing and the overall mechanical properties of the remanufacturing parts possibly can meet or exceed that of new one by the regulation of the microstructure and the mechanical properties of heat affected zone and cladding. In general, as an advanced refabrication technology, laser remanufacturing was widely applied in repairing and regeneration of many high value-added equipment [2–6].

Although laser remanufacturing technology had been widely applied in many industries like aerospace, oil drilling, electricity, automobile and machine, there exist some unsolved problems causing seriously restricted the development and use of this technology. Quite different with the laser additive manufacturing process, the deposition of the alloy powder material was on the surface of the work-piece during the laser remanufacturing and therefore the interface between the cladding and the matrix cannot be neglected. Two specific aspects of the work were completed during the laser remanufacturing. Firstly, the high-density and high mechanical properties cladding part was obtained by the design and control of the laser cladding alloy powder material, the process optimization and the proper postprocessing like stress-relief heat treatment, which is similar to the laser additive manufacturing process. However, the regions adjacent to the surface of the work-piece (the depth of the region was about 100–1000 micrometers according to many studies) experienced different short multicycle with superhigh heating and cooling rate and moreover a series of nonequilibrium solid state phase transformation occurred during the interaction between laser beam and alloy powder material. Consequently, the microstructure of the heat affected zone was different with that of the work-piece before remanufacturing and the mechanical performance may deteriorate, namely thermal damage during the laser remanufacturing. Recently, the 3D print technology had drawn a lot of attention of large enterprises and academic institutions. Studies on the laser additive manufacturing processing optimizing were done by the combination of numerical simulation and experimental methods. Some mechanism of the grain morphology

control was investigated by basic study on solidification nucleation and growth mechanisms of the local melting pool. Most of the studies focused on the pretreatment and heat-treatment during the laser cladding process and it turned out that the microstructure and mechanical properties improved significantly. Consequently, heat affected zone (HAZ) was the weak region for the laser remanufacturing parts and the relevant issues had deep effects on the development of this technology [7–11].

Until now, studies on the mechanism of the microstructure evolution and mechanical properties distribution were sorely lacking. The key parts of the issues were the nonequilibrium phase transformation and the evaluations of the mechanical properties of HAZ. First of all, the regions in different depth in HAZ experienced different thermal cycles and eventually the microstructure and the microhardness of HAZ show a stepwise characteristic. Besides, the microstructure of HAZ may have further changes as the following and continuous heat cycles. For some material systems like martensite stainless steel, a set of characteristic parameters (maximum temperature, heating rate and cooling rate) of the heat cycles in HAZ can be acquired by methods like computer numerical simulation and temperature-measuring technology. To some extent, the formation mechanism of the final microstructure in HAZ can be explained and predicted by the classic phase transformation theory. However, some none-equilibrium microstructure frequently appear in HAZ, which make controlling the microstructure and the mechanical properties challenging. In addition, the mechanical properties evaluation of HAZ was challenging but significant. According to previous studies, by prefabricated delimitation the butt joint specimens were obtained as the mechanical properties tests samples or obtained directly from the laser cladding part along the cladding direction.

2. Solid state phase transformation during the remanufacturing processing of martensite stainless steel

Martensite phase transformation was a displacive phase transformation. During the martensite phase transformation, lattice type were changed by shear of material atoms, as well as the mechanical, thermodynamic properties and specific volume of the material. The thermodynamic and latent heat of phase transformation changes will have massive effects on the evolution of the temperature field.

During the laser cladding, material will experience a complete cycle from room temperature up to melting points. The physical properties of material changed as the occurrence of the solid state phase transformation and then eventually affected the evolution of the temperature field and stress field. The studies on the temperature and stress field evolution during the laser remanufacturing were based on the reveal of physical properties evolution. Furthermore, the heat cycles of different regions in HAZ can be obtained from the temperature field evolution and then the mechanism of the microstructure and mechanical properties distribution in HAZ may be revealed. Last but not the least, we hope the final microstructure and mechanical properties of HAZ can be accurately predicted and well controlled. However, the solid state phase transformation during the laser cladding was a non-equilibrium phase transformation and the kinetics of phase transformation were obviously affected by the superhigh heating rate and cooling rate [12, 13].

2.1. The effects of solid state phase transformation on the specific volume of martensite stainless steel

In the case that no phase transformation occurs for some generic solid material, the temperature rises will increase as the internal energy rises, so is the volume. On the contrary, the temperature and the volume decrease as the internal energy fall.

The specimens of the thermal expansion coefficient measurement were shown as **Figure 1**. The dilatometry experiment was processed in DIL801 dilatometer (**Figure 2**). In the temperature range (−150~1500°C), the maximum heating rate was 50°C/min and the maximum cooling rate was 25°C/min at low temperatures. In addition, the maximum heating rate rise to 100°C/min and the maximum cooling rate reached to 180°C/min as well. The errors of linear expansion coefficient was set as 0.03*10–6/°C, the gradient of temperature was 10°C/min. Using nitrogen as carrier gas, the flow rate was set as 20 ml/°C. The ambient temperature was 25°C and humidity was 35%.

The radial strain of the specimens for the thermal expansion coefficient experiments were used as measurement results. The strain was decomposed into two parts in the Ti (Range from room temperature to Ms): One part were the strain variations of martensite and austenite as temperature changes. The rest were caused by the volume effect of martensite phase transformation. It could be described as follows:

$$\Delta L/L_0 = \beta_M^0 V_i + (1 - V_i)\,\alpha_A\, T_i + V_i\,\alpha_M\, T_i$$

dealed as:

$$\beta_M^0 = (\alpha_\alpha - \alpha_\gamma)\Delta T - \Delta\,\varepsilon_M^{RT}$$

where $\Delta\,\varepsilon_M^{RT}$ are the intercept of the extension line of austenite section during the cooling period in the temperature-strain curves and β_M^0 are the strain caused by the volume effect of solid state phase transformation.

For FV520B high-strength stainless steel, the free expansion curve was shown as **Figure 3**. The critical temperature of transformation from pearlite to austenite (Ac1) was 600°C and the complete transformation temperature of austenite (Ac3) was 900°C. The starting temperature of the martensite phase transformation (Ms) was 130°C.

Figure 1. Specimens for the free dilatometry test.

http://dx.doi.org/10.5772/intechopen.79910

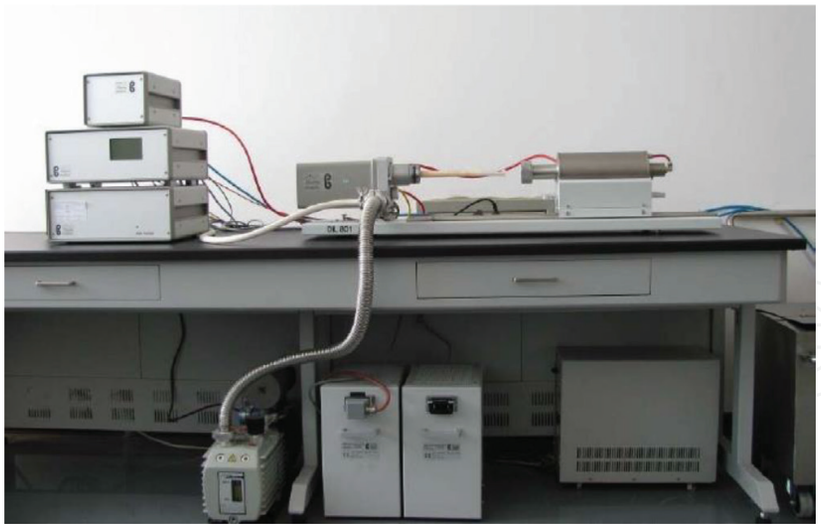

Figure 2. DIL801 single-sample dilatometer.

Shown as **Figure 4**, in the temperature between 130 and 600°C, the strain of martensite was 0.0057 and that of austenite was 0.088. The expansion coefficient of austenite was 18.72 and that of martensite was 12.13. In high temperature, the expansion coefficient of austenite was 21.5 and that of martensite reached up to nearly 19 at temperature over 600°C.

Figure 5 shows the temperature range of martensite transformation during the free dilatometry test. In the martensite phase transformation period, the strain caused by volume effect during phase transformation was 0.0067249 and the real strain should be 0.00328 considering the thermal contraction. Ideally, the material volume increased by 0.97% compared with that at Ms. In addition, the material volume at 320°C was equivalent to that at room temperature.

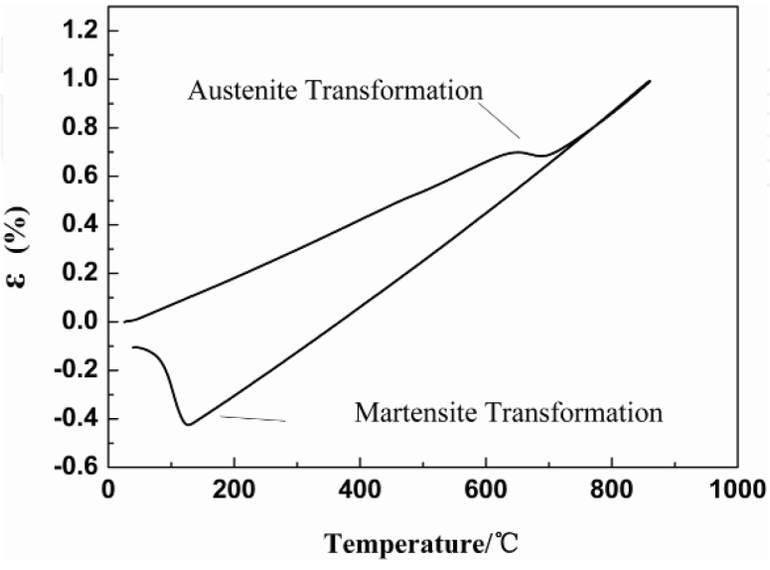

Figure 3. The free dilatometry test of FV520B steel.

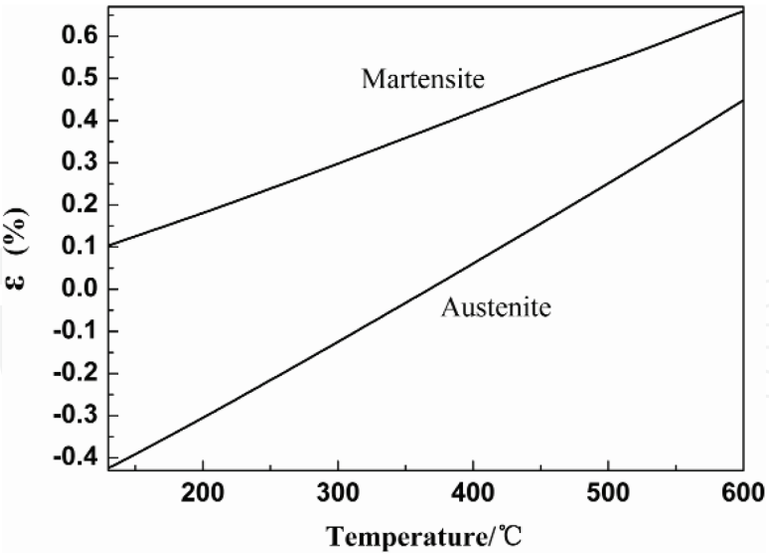

Figure 4. Temperature range of two phase regions during the free dilatometry test.

For materials in the temperature between M_s and A_c line, it could be martensite, austenite or dual-phase structure. The lower was the temperature, the higher was the density contrast of the two phase states. Consequently, the volume effect during phase transformation was more significant and the volume changes increased as the temperature drop. For the solid state phase transformation of the common steel, the transformation temperature of pearlite was the highest, next was bainite and that of martensite was the lowest [9]. In general, the volume effect of these phase transformations were corresponding to the transformation temperatures.

It had been noted above that superhigh heating rate and cooling rate had magnificent impact on the physical parameters of material during the laser remanufacturing. Studies indicates that the heating rate could reached over 500°C by methods of computer numerical simulation

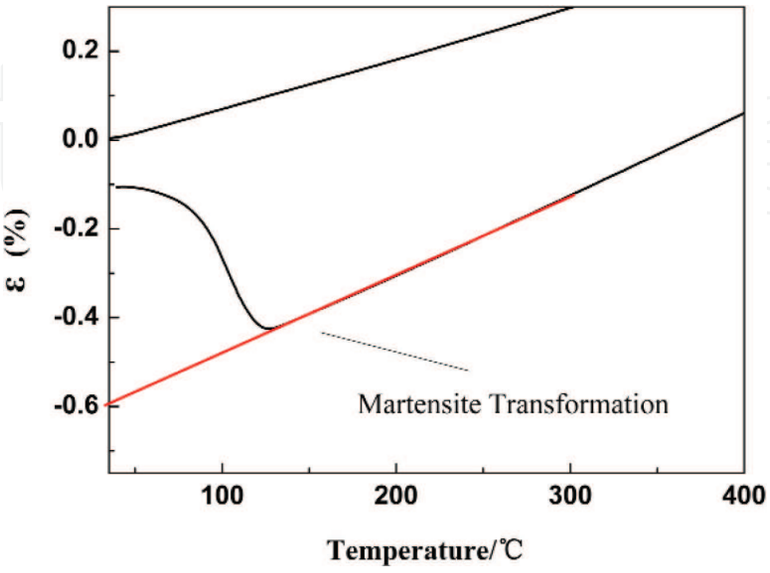

Figure 5. Temperature range of martensite transformation during the free dilatometry test.

http://dx.doi.org/10.5772/intechopen.79910

and temperature measurements. The simulation experiments were designed and conducted to study the effect of heating rate on the solid state phase transformation. Limited to the instrument condition, the heating rates were set as 0.25, 1, 5, 10, 30, 80 and 100°C/s. The results revealed that the rise of heating rates of each thermal cycles significantly increased Ac1 and Ac3 of FV520B (as shown in **Figure 6**). The expansion coefficient of martensite at 640°C increased apparently as the heating rate increased from 5 to 30°C/s. In general, heating rates had a great effect on the kinetics parameters of the austenite phase transformation.

2.2. The thermal cycles of laser cladding FV520B considering the effect of solid state phase transformation

In recent years, many studies were concerned about the effects of solid state phase transformation on the temperature and stress field and the mechanisms were revealed by experimental methods. However, the theoretical analysis were not enough in conditions of the complex projects like laser remanufacturing, which involved process control with many parameters. Therefore, computer numerical simulation was considered as a practical method to obtain precise, comprehensive and quantitative results, which had engineering meanings.

All the involved parameters were listed below: laser power, scanning rate, laser spot size and lapping rate were 1.5KW, 10 mm/s, 3 mm, 50% respectively. Using the technique of deactivate and reactivate element, the cladding material were activated by passes and layers. By building the coupling thermo-mechanical model, the evolution of the temperature field during the cladding was revealed. This work focused on the short and varying thermal cycles in positions with different depth in HAZ during the single-pass and multi-layer claddings. **Figure 7** was the geometries of the laser cladding samples during the single-pass and multi-layer processes [12, 14, 15].

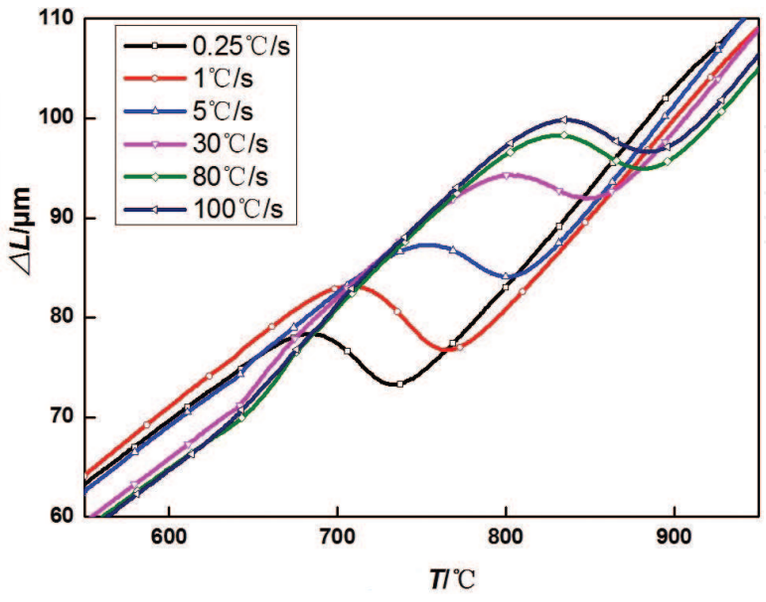

Figure 6. The free dilatometry test of FV520B steel in different level of heating rate.

Figure 8 was the temperature evolution at midpoint of single-pass cladding sample. The temperature of the melting pool reached 1833°C after 3.5 s. Meanwhile, the temperature measurement experiment at the midpoint was conducted by using RaytekMM infrared thermometer. The results showed that the laser beam scan midpoint of the single track after 3.7 s and the temperature of the melting pool was 2175°C, which was consistent with the simulation results.

Figure 9 was the thermal cycles in HAZ during the single-pass cladding. The maximum temperature in regions close to surface of the work-piece reached over 1000°C, which is higher than the complete austenitic temperature Ac3. In addition, the measurement results of the heating rate was around 500°C/s and that of the cooling rate was over 100°C. For regions in different depth of HAZ, the maximum temperatures of the thermal cycles were the main difference, which could directly affected the final microstructure in HAZ. Meanwhile, the simulation results could be provided as evidence for the studies on the mechanism of the microstructure evolution.

Figure 10 was the thermal cycles in HAZ during the multi-layer cladding. In multi-layer laser remanufacturing process, the coating is deposited layer by layer and HAZ was created repeatedly [16]. In addition, the repeatedly thermal effect on microstructure in HAZ was hard to control and predict. Some studies pointed that the microstructure in HAZ experienced approximate tempering during the repeatedly thermal cycles and toughening effect on microstructure was observed. The numerical simulation results showed that microstructure of HAZ experienced thermal cycles with over 600°C maximum temperature during the subsequent deposition process after the first layer cladding. It was considered that the multi-cycle heating and cooling process could affect the final microstructure and mechanical properties in HAZ.

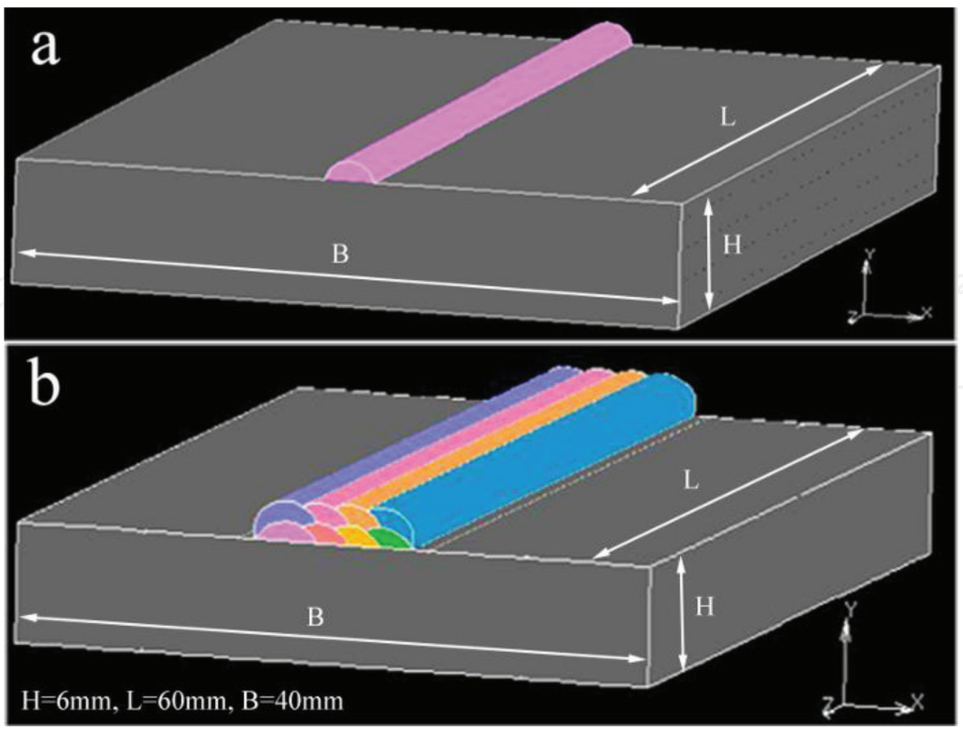

Figure 7. Geometry of laser clad sample: (a) single-layer; (b) multilayer.

http://dx.doi.org/10.5772/intechopen.79910

2.3. The continuous cooling transformation (CCT) curve of FV520B

Figure 11 was the schematic of phase transformation for the martensite stainless steel during

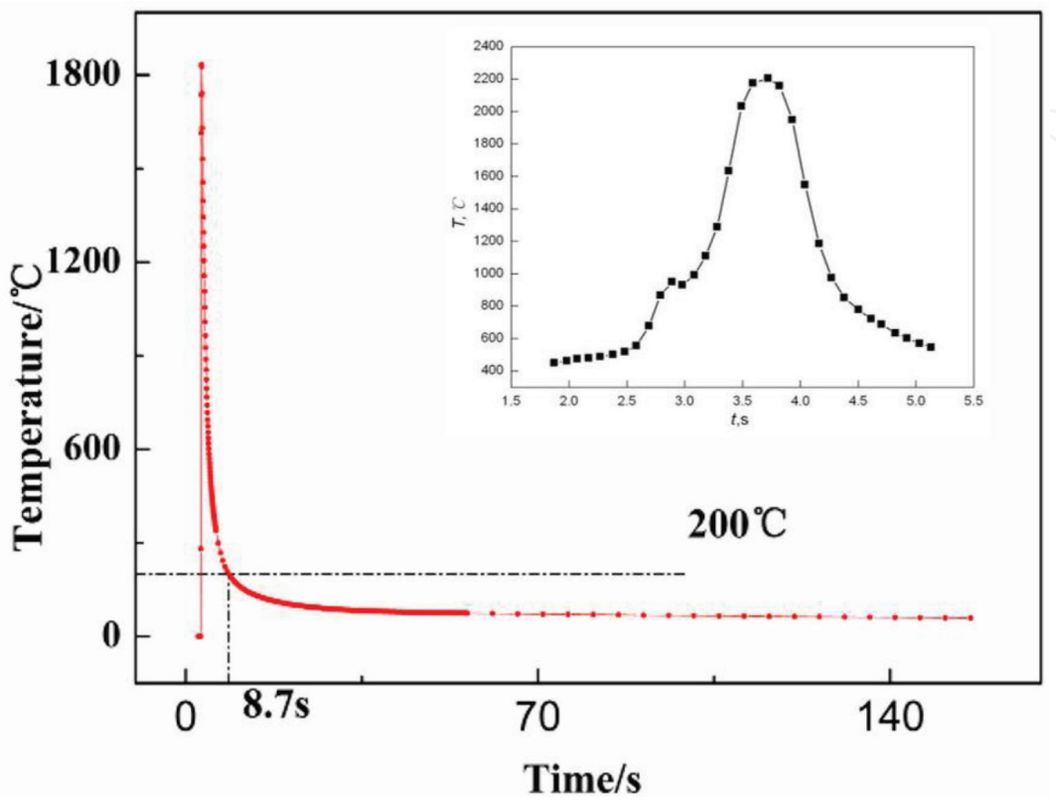

Figure 8. Temperature variation at midpoint of single-layer laser clad sample.

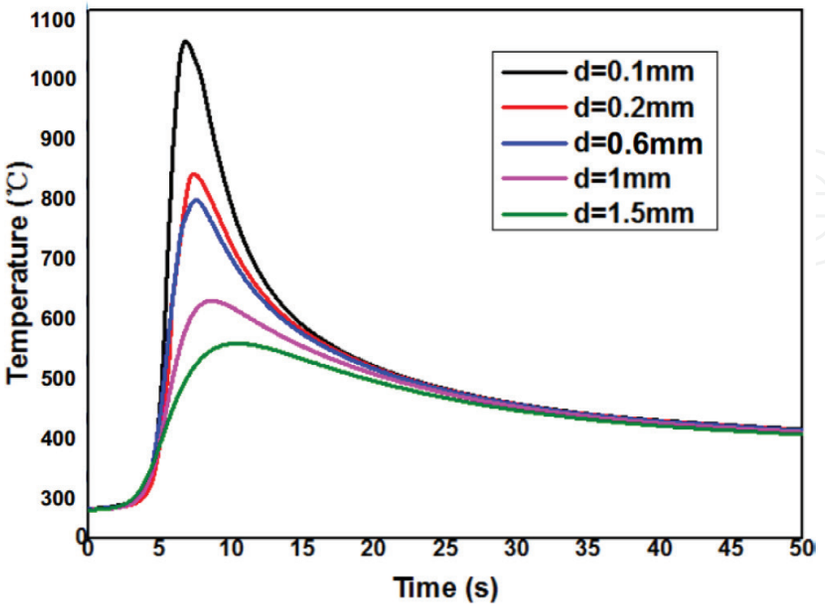

Figure 9. The thermal cycles in HAZ.

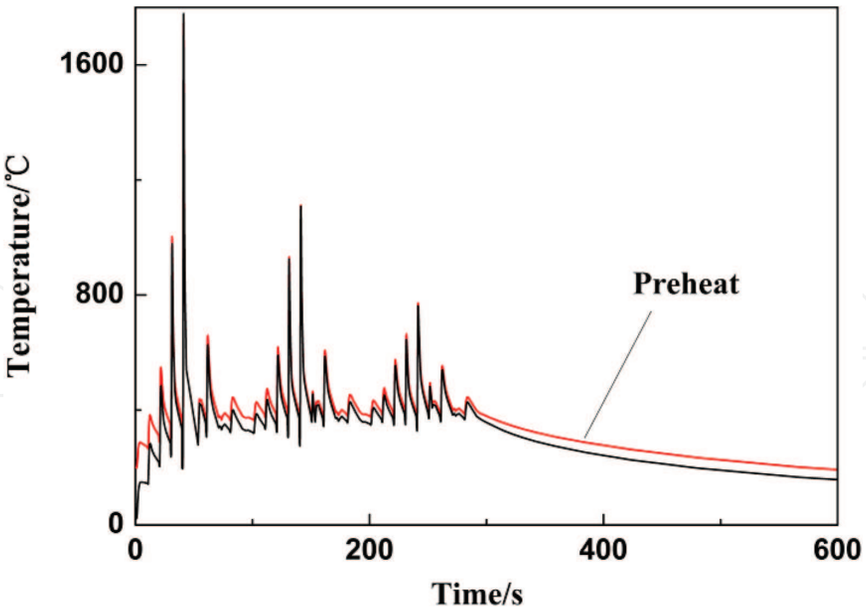

Figure 10. The temperature at the midpoint of the five pass of the first layer, with and without preheating.

the laser remanufacturing process. Austenite was assumed to be the initial phase during solidification process. In addition, the martensite transformation occurred during the cooling process due to the high cooling rates. As temperature decreased, the martensite transformation started at Ms and finished at Mf. When a new layer of FV520B was deposited, the previously deposited material experienced a new thermal cycle. Once the rising temperature was higher than Ac1, the transformation of martensite to austenite occurred. The percentage of austenite phase increased linearly as temperature rise.

As the physical properties of material depended on temperature and phases, the accuracy of the physical properties based on the appropriate description on the evolution of phase. In laser cladding process, different regions had different thermal cycles and external load, which

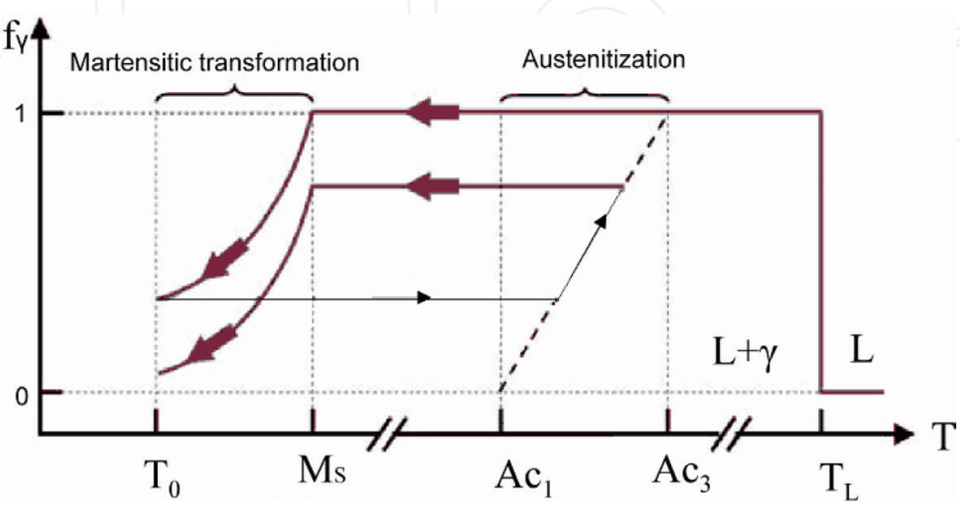

Figure 11. Evolution of volume fraction of austenite during phase transformation during Laser cladding directed shaping.

could contribute to the change of the kinetics and effect of solid state phase transformation. Therefore it was necessary to carry out systematical research in the influence of cooling condition on the solid state phase transformation during the cooling process [17].

A combined experiment by methods of dilatometry and metallography was conducted and the CCT curve was obtained by the L78 RITA transformation measuring apparatus. According to the thermal cycles of the laser cladding processes, two austenitic procedures were designed to study the effect of the austenitization condition on the microstructure evolution. The process of case 1 was designed as below: the sample heated up to 1000°C at heating rate of 300°C/s and kept the temperature for 5 s. In the cooling period, the sample was cooled to 810°C at the cooling rate of 100°C/s, kept the temperature for 5 mins and then was cooled at cooling rate of 0.02, 0.08, 0.2, 0.5, 1 and 50°C/s respectively. For case 2, the sample heated up to 1300°C at the same heating rate, was kept the temperature for 5 s and cooled to 810°C at the same cooling rate. Then, the sample was cooled at cooling rate of 0.02, 0.08, 0.2, 0.5, 1°C/s respectively. The phase transformation temperatures were obtained using tangent method.

Figure 12 was the continuous cooling transformation of FV520B stainless steel. **Figures 13** and **14** were metallograph of microstructures in different austenitic procedures. The results showed that the microstructures were all martensite in the designed cooling parameters due to the hardenability of FV520B stainless steel. For case 1, the microstructure was lath martensite with finely distributed precipitates. In addition, the proportion of martensite with sparse laths increased with the increasing cooling rate in the process. For case 2, the microstructure was lath martensite as well. However, the microstructure of martensite in case 2 was coarser than that of case 1 and dispersedly distributed precipitates were barely observed. As shown in **Figures 15** and **16**, the phase transformation temperature of case 2 was 20°C lower than that of case 1 and both increased as the cooling rate became higher; the microhardness of case 2 was 60 HV higher than that of case 1 and both decreased as the increasing cooling rate. In general, the maximum temperature of thermal cycle had a dominating effect on the microstructure, microhardness and phase transformation temperature rather than cooling rate.

It was considered that the maximum temperature was 1000°C with short heat preservation in case 1 and the sample experienced complete austenitic process with precipitates partly

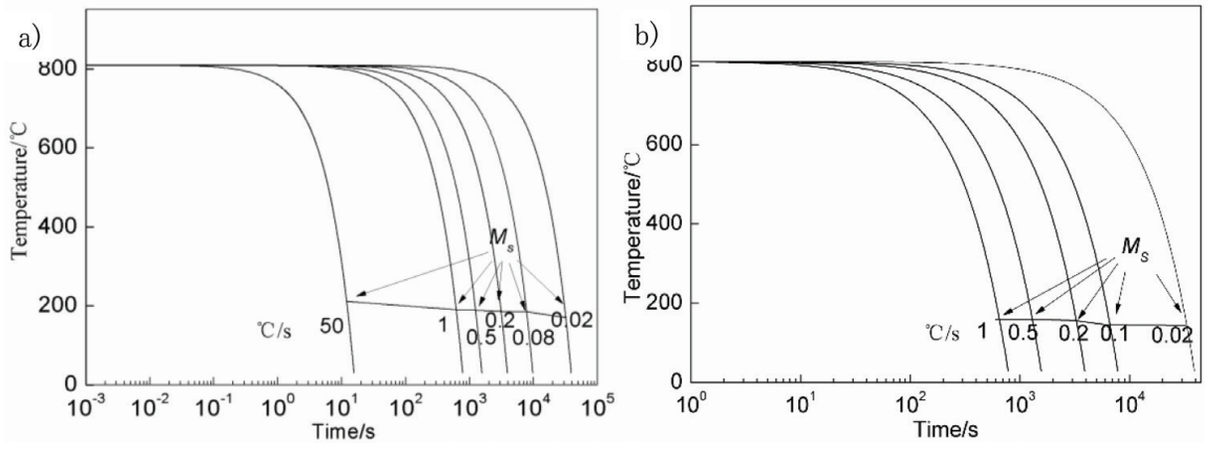

Figure 12. Welding continuous cooling transformation of FV520B stainless steel: (a) Case I; (b) Case II.

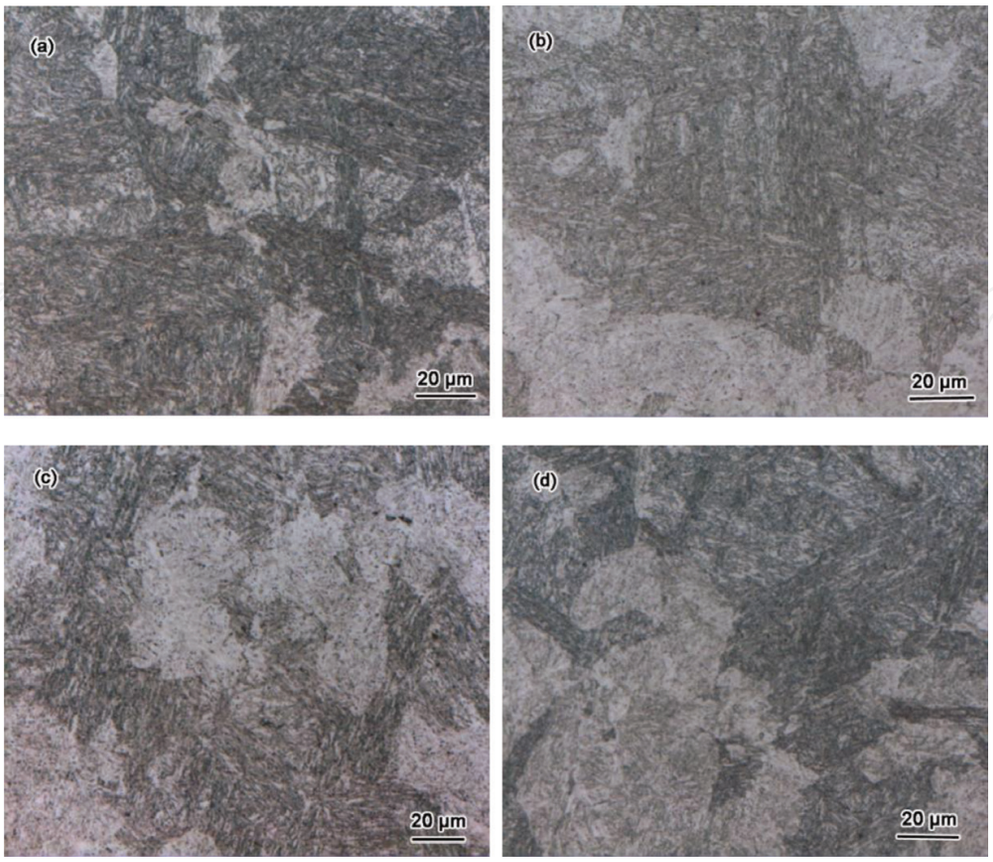

Figure 13. OM images of specimen Case I under different cooling rates. (a) 0.02°C/s; (b) 0.2°C/s; (c) 0.5°C/s; (d) 1°C/s.

dissolving in the matrix. In addition, the precipitates further grew coarse and solubility in the matrix decreased, which eventually contributed to the decreasing microhardness. However, the maximum temperature of case 2 reached 1250°C and no ferrite existed at high temperature. In general, the sample of case 2 experienced complete austenitic process with precipitates completely dissolving in the matrix. The increasing solid solubility of alloy elements contributed to the higher microhardness than that of case 1. Meanwhile, phase transformation temperature of case 1 and case 2 were both low and it could caused by the strengthen effect of austenite and growth of precipitates during the cooling period at low cooling rate.

The microhardness of laser remanufacturing specimens was higher than that from CCT process due to the superhigh heating rate in the actual laser cladding process. According to the numerical simulation results, the temperature gradient in high temperature period reached to 1000°C/s during the laser cladding process and the maximum heating rate could be set as 500°C/s due to the restrictions of instrument condition **Figures 15** and **16**.

As above, austenitic process and cooling rate had a remarkable impact on the phase transformation temperature and it could be interpreted as the effect of thermal cycle on the valid elements of material composition. It was assumed that the maximum temperature and heating rate during the heating period in the thermal cycle had great influence on the martensitic phase transformation temperature. Moreover, the strengthen effect and reducing of Ms took

http://dx.doi.org/10.5772/intechopen.79910

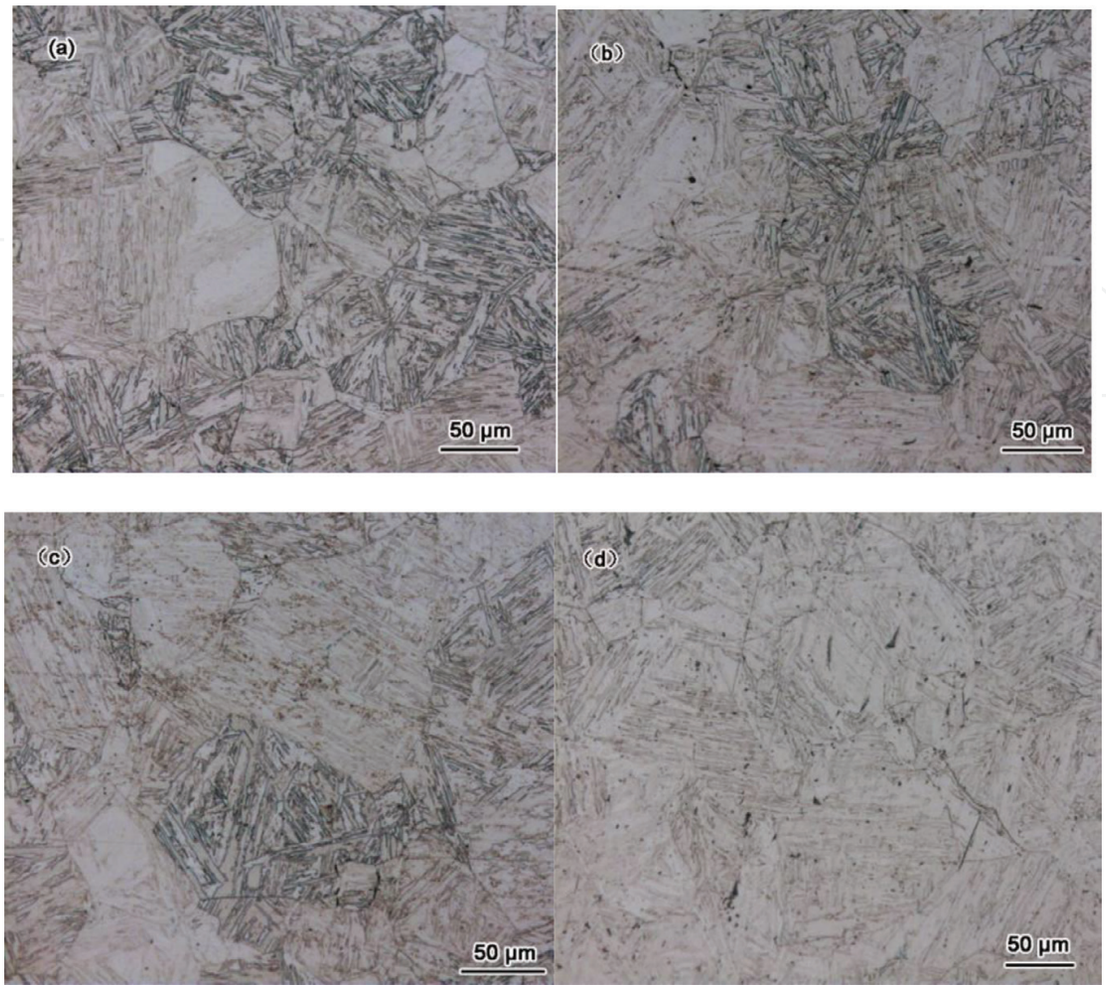

Figure 14. OM images of specimen Case II under different cooling rates. (a) 0.02°C/s; (b) 0.2°C/s; (c) 0.5°C/s; (d) 1°C/s.

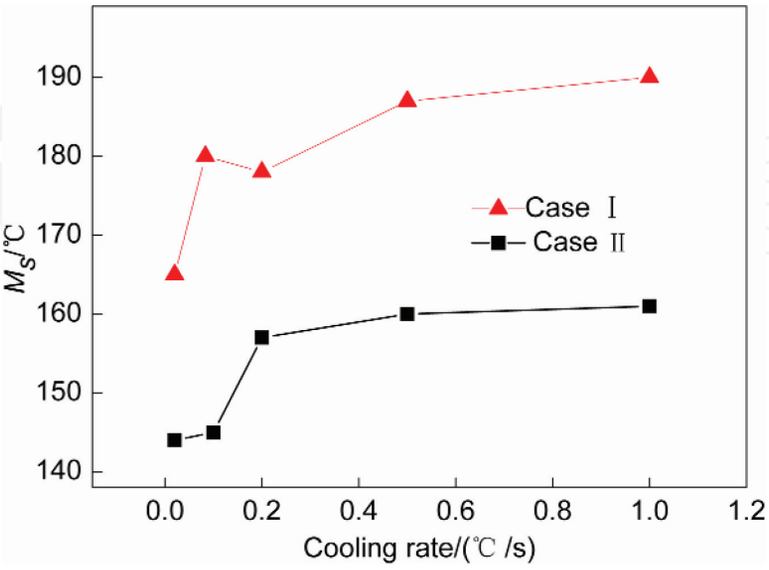

Figure 15. Martensite transformation start temperature under Case I and Case II.

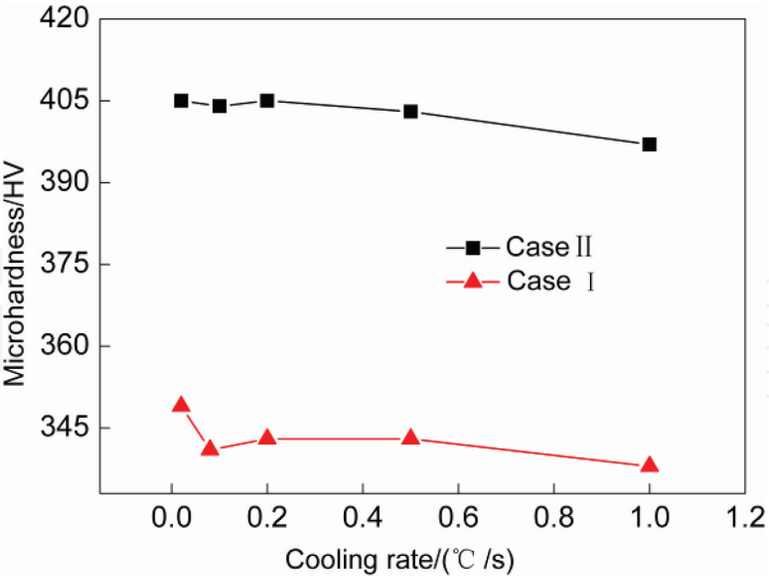

Figure 16. Hardness under the Case I and Case II.

place due to the low cooling rate during the same austenitic process. In general, the thermal cycles had a significant effect on the metallographic transformation [18, 19].

3. The Microstructure characteristics in HAZ of laser remanufacturing FV520B

Figure 17 were microstructure distribution of HAZ. It could be seen that the HAZ microstructure showed a stepwise characteristic. The microstructure of regions adjacent to interface was coarse martensite and no ferrite existed in high temperature. In thermal cycles of these regions, it experienced complete austenitic phase transformation and precipitates fully dissolved in the matrix and consequently the final microstructure of the regions were martensite with less lath characteristics. In the middle area of HAZ where the maximum temperature of the thermal cycle was close to Ac3 and the matrix underwent the complete austenitic as well. For the partially austenization zone, the laser energy input was relatively low and the matrix experienced partially austenization due to a thermal cycle with a maximum temperature between Ac1 and Ac3. Therefore, the microstructure was lath martensite with more dispersedly distributed precipitate and particles. The microstructure of regions in the bottom of HAZ was similar to the original microstructure of FV520B and it was considered to undergo the thermal cycle with a maximum temperature near Ac1.

Figure 18 was the microhardness distribution of cladding layer, HAZ and substrate. The microhardness distribution was considered consistent with that of microstructure. In the complete melting zone where the maximum temperature of thermal cycle was higher than AC3, it showed high hardness due to the solution strengthen. In the partially austenization zone, the microhardness was lower than other regions.

http://dx.doi.org/10.5772/intechopen.79910

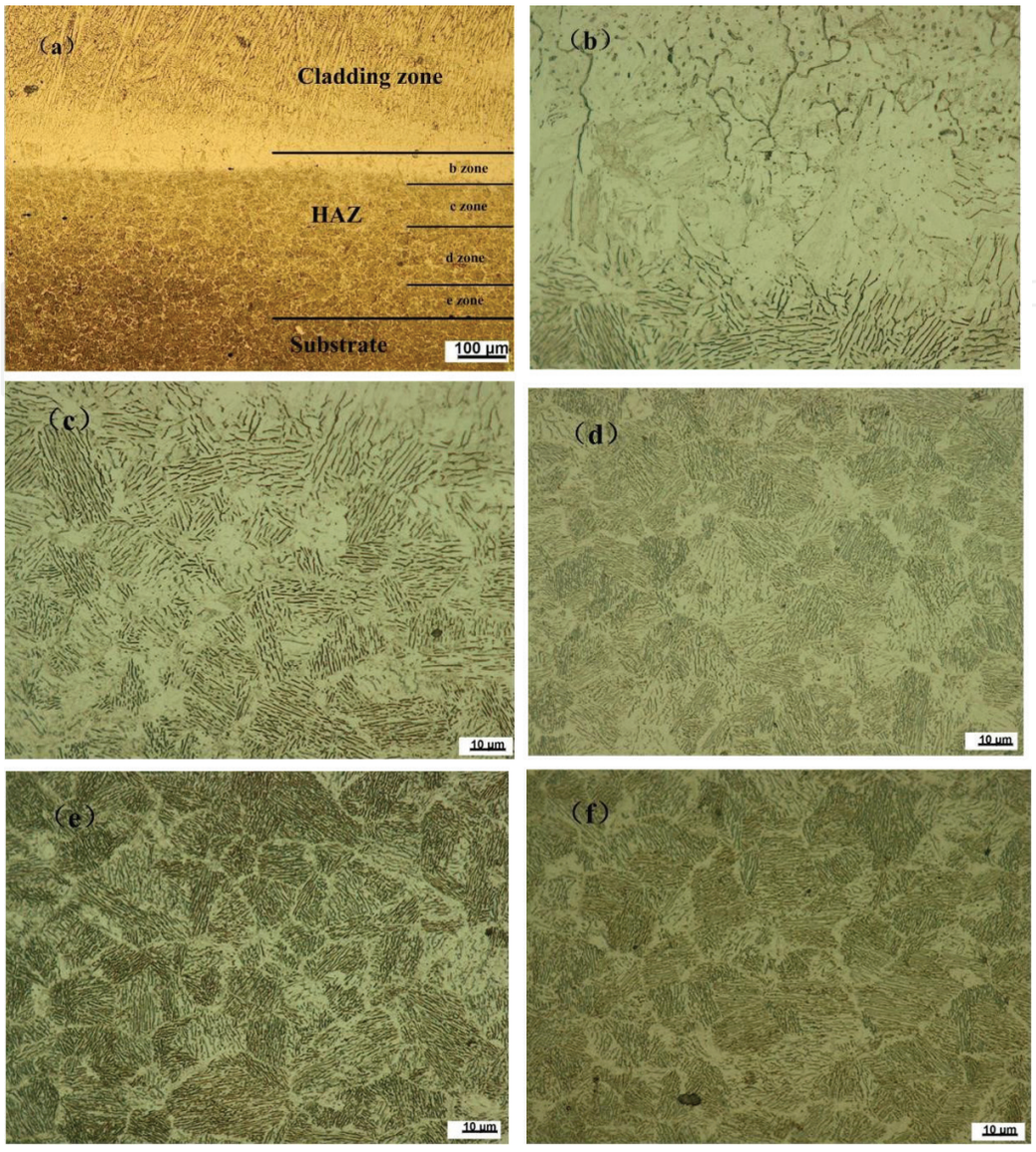

Figure 17. OM images of laser RM FV520B: (a) Macrostructure of laser RM FV520B (b) region close to the interface (c) partially molten zone (d) completely austenization zone (e) partially austenization zone (f) FV520B substrate.

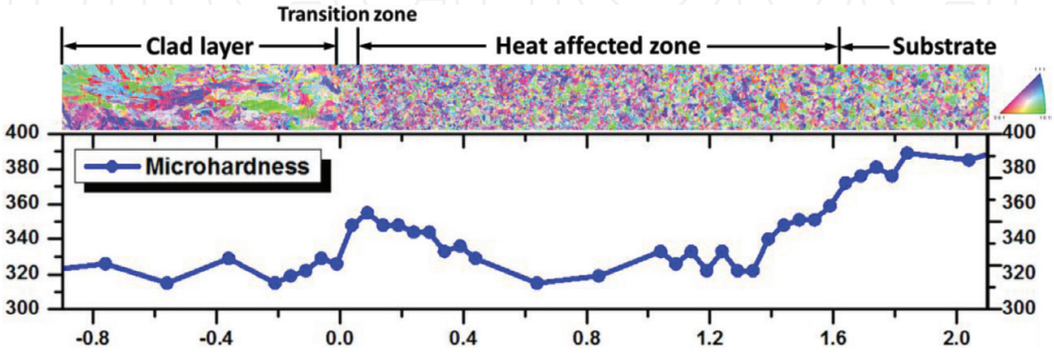

Figure 18. Microhardness distribution of HAZ-substrate.

4. Mechanical properties of laser remanufacturing FV520B

Figure 19 was the tensile test results of FV520B steel and cladding layer of laser remanufacturing FV520B. It could be seen that the yield stress, tensile stress and elongation of FV520B steel were respectively 830 Mpa, 970 Mpa and 23% and that of FV520B laser cladding layer were 920 Mpa, 1280 Mpa and 11% respectively. The results indicated that the strength of alloy increased and ductility decreased after laser remanufacturing process.

Figure 20 was the tensile test curves of laser remanufacturing butt samples and FV520B steel samples. The results showed that two samples had similar stress–strain curve. It could

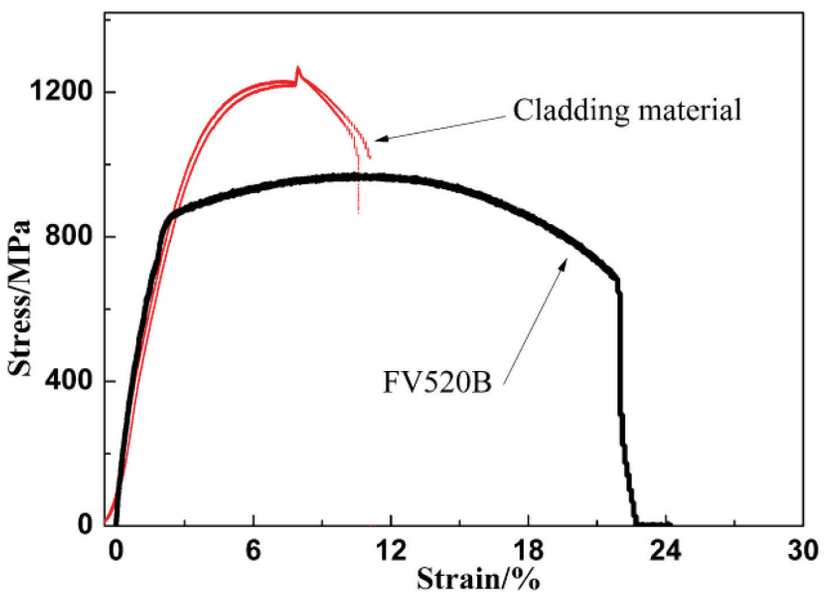

Figure 19. Comparison of tensile test curves between FV520B steel and as-deposited component.

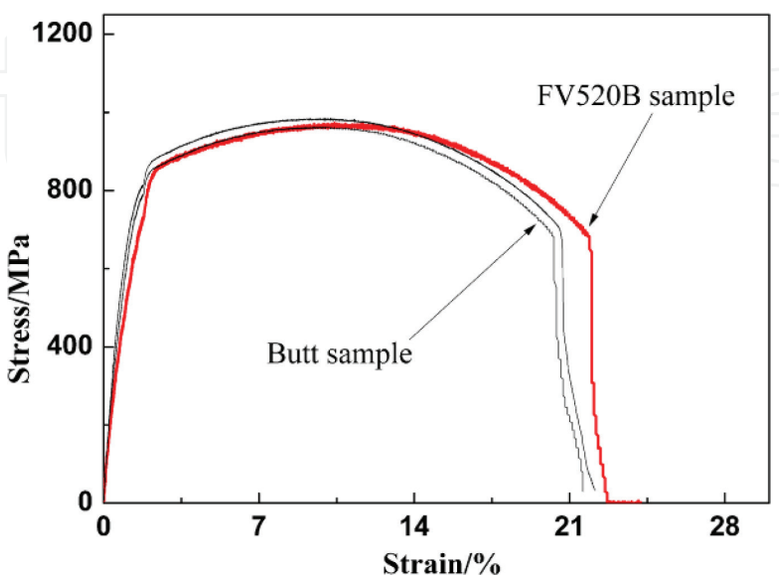

Figure 20. Comparison of tensile test curves between FV520B steel and butt sample.

http://dx.doi.org/10.5772/intechopen.79910

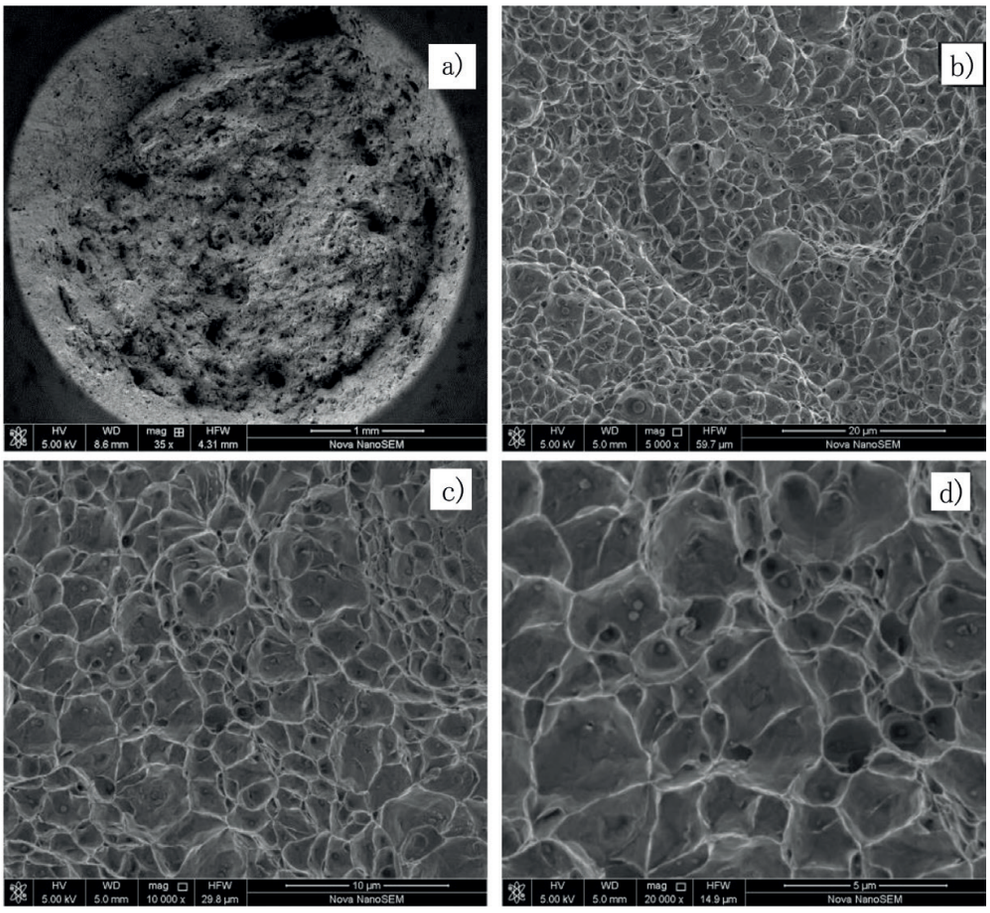

Figure 21. Fracture surface morphologies of FV520B steel fabricated by laser cladding. (a) Macro morphology of fracture surface; (b) fracture surface by 5000 times; (c) fracture surface by 10,000 times; (d) fracture surface by 20,000 times.

be predicted that the fracture section of butt samples was the bottom of HAZ due to the strengthen and descend of ductility of HAZ after laser remanufacturing process. In this research, FV520B work-piece underwent aging treatment after forging process and showed relative low strength but high ductility. In general, laser remanufacturing FV520B had high strength and ductility, which reached the combination properties of forgings.

Figure 20 was the fracture surface morphologies of laser remanufacturing FV520B samples. Ductile characteristics were observed without any apparent flaws or inclusion. In addition, High density and tiny dimples were observed at high magnification, where nanoscale spherical particles were founded. In general, the results showed that the material had good ductility with uniform distribution of nanoscale particles and no segregation at grain boundaries **Figure 21**, crack or inclusion were founded in the fracture surface [20].

5. Conclusions

Laser remanufacturing is an advanced repairing method to remanufacture damaged parts based on laser cladding processing. To reveal the mechanism of solid state phase transformation and the microstructure evolution during the laser cladding processing, it is necessary to

study the effect of solid state phase transformation on physical properties and temperature filed by numerical simulation and experimental method. For FV520B stainless steel, the result of free dilatometry test showed that heating rates had a great effect on the kinetics parameters of the austenite phase transformation and the volume effect of phase transformations were corresponding to the phase transformation temperatures. According to the results of thermal simulation experiment and metallographic observation, it was considered that the multi-cycle heating and cooling process affected the final microstructure and mechanical properties in HAZ. The maximum temperature of thermal cycle had a dominating effect on the microstructure, microhardness and phase transformation temperature rather than cooling rate. Thermal cycle influenced significantly the metallographic transformation and consequently decided the final mechanical performance. By using the optimal process, laser remanufacturing FV520B had high strength and ductility, which reached the combination properties of forgings.

Acknowledgements

The work was supported by the National Key Research and Development of China (Grant No. 2016YFB1100205), and 973 Project of China (Grant No. 2011CB013403).

Author details

Shi-yun Dong*, Xiang-yi Feng, Jin-xiang Fang and Shi-xing Yan

*Address all correspondence to: syd422@sohu.com

National Key Laboratory for Remanufacturing, Academy of Armored Force Engineering, Beijing, China

References

[1] Wang HM. Materials' fundamental issues of laser additive manufacturing for high-performance large metallic components. Acta Aeronautica at Astronautica Sinica, China. 2014;**35**(10):2690-2693. DOI: 10.7527/S1000-6893.2014.0174

[2] Xu BS. Theory and Technology of Equipment Remanufacturing Engineering. Beijing, China: National Defense Industry Press; 2007

[3] Walsh B. PSS for product life extension through remanufacturing. CIRP IPS2 Conference, Sweden: Linköping University Electronic Press; 2010:261-266

[4] Xu BS, Dong SY. Laser Remanufacturing Technology. Beijing, China: National Defense Industry Press; 2016

[5] Lund RT. The Remanufacturing Industry: Hidden Giant. Boston, Massachusetts: Boston University; 1996

[6] Nasr N, Thurston M. Remanufacturing: A Key Enabler to Sustainable Product Systems. Rochester, NY-USA: Rochester Institute of Technology; 2006

[7] Qiu CL, Ravi GA, Dance C, et al. Fabrication of large Ti-6Al-4V structure by direct laser deposition. Journal of Alloys and Compounds. 2015;**629**:351-361. DOI: DOI 10.1016/j.jallcom.2014.12.234

[8] Mower TM, Long MJ. Mechanical behavior of additive manufactured, powder-bed laser-fused materials. Materials Science and Engineering A. 2016;**651**:198-213. DOI: 10.1016/j.msea.2015.10.068

[9] Yadollahi A, Shamsaei N, Thompson SM. Effects of process time interval and heat treatment on the mechanical and microstructural properties of direct laser deposited 316L stainless steel. Materials Science and Engineering. 2015;**644**:171-178. DOI: 10.1016/j.msea.2015.07.056

[10] Wang T, Zhu YY, Zhang SQ, et al. Grain morphology evolution behaviour of titanium alloy components during laser melting deposition additive manufacturing. Journal of Alloys and Compounds. 2015;**632**:505-513. DOI: 10.1016/j.jallcom.2015.01.256

[11] Goldak JA, Akhlaghi M. Computational Welding Mechanics [M]. New York: Springer US; 2006

[12] Costa L, Vilar R, Reti T, et al. Rapid tooling by laser powder deposition: Process simulation using finite element analysis. Acta Materialia. 2005;**53**(14):3987-3999. DOI: 10.1016/j.actamat.2005.05.003

[13] Xu ZY. Martensitic Transformation and Martensite. Beijing, China: Science Press; 1999

[14] Francis JA, Bhadeshia H, Withers PJ. Welding residual stresses in ferritic power plant steels. Materials Science and Technology. 2007;**23**(9):1009-1020. DOI: 10.1179/174328407X213116

[15] Börjesson L, Lindgren LE. Simulation of multi-pass welding with simultaneous computation of material properties. Journal of Engineering Materials and Technology. 2001;**123**(1):106-111

[16] Chen Y, Zhang K, Huang J, et al. Characterization of heat affected zone liquation cracking in laser additive manufacturing of Inconel 718. Materials and Design. 2016;**90**:586-589. DOI: DOI 10.1016/j.matdes.2016.10.155

[17] Koistinen DP, Marburger RE. A general equation prescribing the extent of the austenite-martensite transformation in pure iron-carbon alloys and plain carbon steels. Acta Metallurgica. 1959;**7**(1):59-60

[18] Fang JX, Dong SY, Wang YJ, et al. The effects of solid-state phase transformation upon stress evolution in laser metal powder deposition. Material and Design. 2015;**87**:807-814. DOI: 10.1016/j.matdes.2015.08.061

[19] Xu BS, Fang JX, Dong SY, et al. Heat-affected zone microstructure evolution and its effects on mechanical properties for laser cladding FV520B stainless steel. Acta Metallurgica Sinica. 2016;**52**(1):1-6. DOI: 10.11900/0412.1961.2015.00489

[20] Fang JX. Effects of solid-state phase transformation upon stress evolution during laser cladding forming of martensitic stainless steel. Harbin Institute of Technology; 2016

IntechOpen